Available online at www.sciencedirect.com
ScienceDirect
Journal of Power Sources 161 (2006) 849–855
JOURNAL OF POWER SOURCES
www.elsevier.com/locate/jpowsour

Dynamic numerical simulation of a molten carbonate fuel cell

Hongliang Hao *, Huisheng Zhang, Shilie Weng, Ming Su

The Key Lab. of Power Machinery and Engineering of Education Ministry, Shanghai Jiao Tong University, Shanghai 200030, PR China

Received 20 March 2006; received in revised form 26 April 2006; accepted 27 April 2006
Available online 23 June 2006

Abstract

The paper presents a set of two-dimensional molten carbonate fuel cell mathematical models, considering the electrical, mass and heat transfer characteristics of a molten carbonate fuel cell. A dynamic simulation model was built under the VC++ environment. The steady state and dynamic simulation results for a cross-flow molten carbonate fuel cell were obtained using the simulation model. The results are appropriate for the design and operation of molten carbonate fuel cells.

Keywords: Dynamic; Simulation; MCFC

1. Introduction

A fuel cell is considered as a good candidate for the next generation power source. Fuel cell-based power plants convert chemical energy directly to electricity without the requirement for conversion of energy into heat. In addition, NO_x and SO_x emissions are greatly reduced in comparison with fossil fuel-based generation systems [1,2].

Among the various fuel cell types, the molten carbonate fuel cell (MCFC) is a very promising type, which is now about to become commercially used. MCFCs belong to the high temperature fuel cell class: the operating temperature range is about 600–700 °C, in which the electrolyte has a good ionic conductivity [3]. The MCFC is considered to be a second-generation fuel cell. It has high efficiency and low emissions of NO_x and SO_x. The MCFC has been proposed in recent years as an extremely efficient solution in power generation.

The distribution parameters, such as the reaction temperature, current density and gas species concentration, have important effects on the operation of the fuel cell. So they will have a very important significance in predicting the distribution of temperature, current density and species concentration in a fuel cell stack. Considering the electrical and heat characteristics of a fuel cell, the paper presents a two-dimensional dynamic mathematical model of the MCFC. The steady and dynamic simulation results of a cross-flow molten carbonate fuel cell were obtained using the simulation model.

2. Working principles of a MCFC

The working principle of a fuel cell is the simultaneous reduction of an oxidant and oxidant of a fuel. Any oxidant gas containing oxygen and carbon dioxide is supplied to the cathode. There the oxygen reacts with carbon dioxide forming carbonate ions. These ions are transported towards the anode where they are involved in the oxidation reaction of hydrogen. At the anode, water and carbon dioxide are formed. The anode reaction produces electrons, while at the cathode, electrons are consumed. The electrons pass from the fuel electrode to the oxidant electrode via an external circuit, and the electrical circuit is completed by ions crossing through an electrolyte. The layout of the MCFC is showed in Fig. 1.

At the fuel cell electrodes, the following electrochemical reactions occur: [5]

At the cathode:

$$\tfrac{1}{2}O_2 + CO_2 + 2e^- \Rightarrow {CO_3}^{-2} \quad (1)$$

At the anode:

$$H_2 + {CO_3}^{-2} \Rightarrow H_2O + CO_2 + 2e^- \quad (2)$$

* Corresponding author. Tel.: +86 21 64477748; fax: +86 21 64470679.
E-mail address: hhler@sina.com.cn (H. Hongliang).

0378-7753/$ – see front matter © 2006 Elsevier B.V. All rights reserved.
doi:10.1016/j.jpowsour.2006.04.109

Nomenclature

E	cell potential (V)
F	faraday constant (c mol^{-1})
h	enthalpy (kJ kg^{-1})
i	local current density (A m^{-2})
K	equilibrium constant
$\vec{n}$	stoichiometric reaction number
Δn	molar flow rate change (mol m^{-3} s^{-1})
ΔP	pressure drop (bar)
q	Generation heat (kJ m^{-3} s^{-1})
Q	reaction heat (kJ kg^{-1})
R_{local}	internal resistance (Ω m^2)
$\vec{R}$	mass rate
ΔS	entropy change of the reaction (J mol^{-1} K^{-1})
T	temperature (K)
V	working voltage of fuel cell (V)
ΔV	local voltage losses (V)
W	power (kW)
y	mole concentration (mol mol^{-1})
η	polarization resistance (Ω m^2)

Subscript

A	anode
C	cathode
E	electrode
MCFC	molten carbonate fuel cell
S1	up separator
S2	down separator
sh	shift reaction

The overall electrochemical reaction:

$$H_2 + \tfrac{1}{2}O_2(g) + CO_{2(C)}(g) = H_2O(g) + CO_{2(A)} \quad (3)$$

There are many processes in the fuel cell, including heat generation and transfer, mass-transfer, oxidation, ionization, reformation and so on. Electro-chemical reactions can produce heat. Meanwhile there is mass-transfer between the gas of anode or cathode and the electrolyte, which forms a mass flow along with a heat flow. And when the current flows through fuel cell, this produces resistance heating due to the various resistances. The heat transfers between the gas and solid parts by conduction, convection and radiation. It will cause a change in the fuel cell's temperature field. At the same time, the temperature distribution also affects the electrochemical reaction.

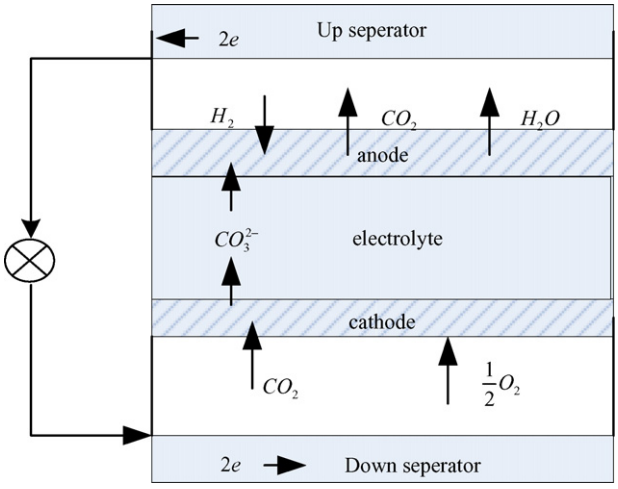

Fig. 1. MCFC schematic.

It can be seen that the thermal physical and electrochemical processes are interactive and interdependent in the fuel cell. The distribution of temperature has a great effect on the electrochemical reaction. So the analysis of heat generation and transfer in a fuel cell is important.

3. Mathematical model for the MCFC

Several assumptions as following are applied in this paper:

(1) The gas flow is in smooth-walled channels of constant cross section.
(2) Cell voltage has no distribution and is constant.
(3) The electrolyte, anode and cathode are considered as a whole, they have the same temperature and character at the same position.
(4) The fuel cell wall is completely insulated, and heat loss is neglected.
(5) The cell is with cross-flow in which fuel gas is in the x-direction and oxidant gas is in y-direction.
(6) The calculated infinitesimal is orthogonal.

$$x = 1, \ldots, j, \ldots, N, \qquad y = 1, \ldots, k, \ldots, M$$

3.1. Power-generation characteristics

The electrochemical reactions are considered to be very fast, and modeled in a steady-state form.

The cell-unit performance of the electricity generation is expressed as: [6]

$$V = E - \Delta V_{\text{ohmic}} - \Delta V_{\text{anode}} - \Delta V_{\text{cathod}} \quad (4)$$

where V (V) is the cell operating voltage, E (V) the reversible local cell potential, ΔV_{ohmic} the local voltage losses due to the internal ohmic resistance, ΔV_{anode} and ΔV_{cathod} are the local voltage losses due to an overpotential at the anode and cathode, respectively, R_{ohm} the internal resistance, and η_{anode} and η_{cathode} are the polarization resistance at the anode and cathode, respectively.

According to the Nernst equation:

$$E = E^0 + \frac{RT}{2F}\ln\frac{y_{H_2} \times y_{O_2}^{0.5} \times y_{CO_2(c)}}{y_{H_2O} \times y_{CO_2(A)}} + \frac{RT}{2F}\ln P \quad (5)$$

where E^0 is the standard potential, P (bar) is the gas pressure.

$$R_{\text{local}} = (R_{\text{ohm}} + \eta_{\text{anode}} + \eta_{\text{cathode}})\,(\Omega\,\text{m}^2)$$

$$V = E - i \times (R_{\text{ohm}} + \eta_{\text{anode}} + \eta_{\text{cathode}})\,(\text{V}) \quad (6)$$

Internal cell resistance is usually expressed by means of an Arrhenius equation as a function of temperature [4]:

$$R_{\text{ohm}} = 0.5 \times 10^{-4} \times \exp\left[3016\left(\frac{1}{T} - \frac{1}{923}\right)\right] \quad (7)$$

$$\eta_{\text{anode}} = 2.27 \times 10^{-9} \times \exp\left(\frac{6435}{T}\right) P_{\text{H}_2}^{-0.42} P_{\text{CO}_2}^{-0.17} P_{\text{H}_2\text{O}}^{-1.0} \quad (8)$$

$$\eta_{\text{cathode}} = 7.505 \times 10^{-10} \times \exp\left(\frac{9289}{T}\right) P_{\text{O}_2}^{-0.43} P_{\text{CO}_2}^{-0.09} \quad (9)$$

It can be seen that the distribution of temperature has direct effect on local potential and resistance from above formulas.

3.2. Conservation of chemical species

During electrochemical reactions, two mole electrons are generated with one mole H_2 at the anode, and consuming a half mole O_2 and one mole CO_2 at the cathode.

The consumption or liberation flow rate $\vec{m}$ (mol m^{-2}s^{-1}) of the gas species H_2, N_2, CO, CO_2, O_2 and H_2O is related to the local current i (A m^{-2}) generation:

$$\vec{m} = \vec{n} \cdot \frac{i}{2F} \quad (10)$$

$$\vec{m} = (m_{\text{H}_2}, m_{\text{N}_2}, m_{\text{CO}}, m_{\text{CO}_2}, m_{\text{O}_2}, m_{\text{H}_2\text{O}})\,(\text{l})$$

where F is the Faraday constant (96493 c mol^{-1}); i the local current density, and $\vec{n}$ stand for the stoichiometric reaction number of individual gas species.

In the fuel gas, the water-shift reaction takes place:

$$\text{H}_2 + \text{CO}_2 \Leftrightarrow \text{H}_2\text{O} + \text{CO} \quad (11)$$

The composition change Δn_{shift} (mol m^{-3} s^{-1}) due to the shift reaction is determined by the local fuel gas concentration. The reaction is double direction.

These chemical processes are very fast on a time scale of 10 μs. They are fast processes compared to the heat flow in a fuel cell. Moreover, volume effect of infinitesimal was considered very small. Therefore, it is reasonable that the electrochemical processes are modeled in steady-state form.

3.2.1. Conservation equation of chemical species for the anode gas

For the anode gas

$$(F_{j-1} + \sum R_i) \times y_j = F_{j-1} \times y_{j-1} + \vec{R}_i \quad (12)$$

where:

$$\vec{R}_i = \Delta n_{\text{shift}} \times \vec{n}_{\text{shift}} \times V + \frac{i}{2\text{F}} \times \vec{n}_{\text{anode}} \times A_{\text{surface}}$$

$$\vec{n}_{\text{shift}}(\text{H}_2, \text{CO}, \text{CO}_2, \text{H}_2\text{O}) = (1, -1, 1, -1)$$

$$\vec{n}_{\text{anode}}(\text{H}_2, \text{CO}, \text{CO}_2, \text{H}_2\text{O}) = (-1, 0, 1, 1)$$

3.2.2. Conservation of chemical species for the cathode gas

For the cathode gas

$$(F_{k-1} + \sum R_i) \times y_k = F_{k-1} \times y_{k-1} + \vec{R}_i \quad (13)$$

where:

$$\sum R_i = -\frac{3i}{4F} \times \Delta Y \times \Delta X$$

$$\vec{R}_i = \frac{i}{2F} \times \vec{n}_{\text{cathode}} \times A_{\text{surface}}$$

$$\vec{n}_{\text{cathode}}(\text{N}_2, \text{O}_2, \text{CO}_2, \text{H}_2\text{O}) = (0, \tfrac{-1}{2}, -1, 0)$$

3.3. Conservation of energy for fuel cell

The study of heat generation and transfer in fuel cell is most important because it has a close relation to the electrochemical reaction rate and power-generation characteristics.

The heat generation in the cell unit arises from three aspects: the electrochemical reaction, the cell losses and the shift reaction.

The local heat generation in the cell unit arises from the electrochemical reaction and cell losses q_e (kJ m^{-3} s^{-1}):

$$q_e = \frac{i \times (-(T\,\Delta S/2F) + ((E - V)/1000))}{t_{\text{cell}}} \quad (14)$$

where ΔS is the entropy change of the reaction, t_{cell} (m) is the thickness of the cell unit.

The heat generation due to water-shift reaction is q_s:

$$q_s = \Delta H_{\text{shift}} \times \Delta n_{\text{CO}}\,(\text{kJ m}^{-3}\,\text{s}^{-1}) \quad (15)$$

where, ΔH_{shift} is the enthalpy change of the shift reaction and Δn_{CO} (mol m^{-3} s^{-1}) is the molar flow rate change in the fuel gas volume unit.

3.3.1. The energy equation for fuel and oxidant gas

The general equation is expressed as:

$$\frac{\partial(\rho \times h)}{\partial \tau} + \text{div}\left(\rho \times \vec{V} \times h - \frac{\lambda\,\nabla h}{C_p}\right) = S_h \quad (16)$$

The up-wind difference equation of the fuel gas in X direction:

$$\begin{aligned}\Delta X \times \Delta Y \times H_A \times \frac{P}{R \times T_j} \times Cp_j \times \frac{\text{d}T_j^A}{\text{d}\tau} &= F_{j-1} \times Cp_{j-1} \times T_{j-1}^A - (F_{j-1} + \sum R_i) \times Cp_j \\ &\times T_j^A + A_{EA} \times K_{EA} \times (T_j^E - T_j^A) + A_{SA} \times K_{SA} \\ &\times (T_j^{S1} - T_j^A) + q_s \times \Delta X \times \Delta Y \times H_A + \frac{i}{2F} \times A \\ &\times Cp \times T_j^E + \frac{i}{2F} \times A \times Cp \times T_j^E \\ &- \frac{i}{2F} \times A \times Cp_{H_2} \times T_j^A \end{aligned} \quad (17)$$

The up-wind difference equation of the fuel gas in Y direction:

$$\begin{aligned}\Delta X \times \Delta Y \times H_{\mathrm{C}} \times \frac{P}{R \times T_k} \times Cp_k \times \frac{\mathrm{d}T_k^{\mathrm{C}}}{\mathrm{d}\tau} &= F_{k-1} \times Cp_{k-1} \times T_{k-1}^{\mathrm{C}} - (F_{k-1} + \sum R_i) \\ &\times Cp_k \times T_k^{\mathrm{C}} + A_{\mathrm{EC}} \times K_{\mathrm{EC}} \times (T_k^{\mathrm{E}} - T_k^{\mathrm{C}}) + A_{\mathrm{SC}} \\ &\times K_{\mathrm{SC}} \times (T_k^{\mathrm{S2}} - T_k^{\mathrm{C}}) - \frac{i}{4\mathrm{F}} \times \Delta X \times \Delta Y \times Cp \\ &\times T_k^{\mathrm{C}} - \frac{i}{2F} \times \Delta X \times \Delta Y \times Cp \times T_k^{\mathrm{C}} \end{aligned} \tag{18}$$

3.3.2. The energy equation for fuel cell (including: electrolyte, anode and cathode) and separators (including: up and down)

$$\rho \times C_{\mathrm{p}} \times \frac{\partial T}{\partial \tau} - \left(\lambda_x \times \frac{\partial^2 T}{\partial x^2} + \lambda_y \times \frac{\partial^2 T}{\partial y^2} + \lambda_z \times \frac{\partial^2 T}{\partial z^2}\right) = q \tag{19}$$

The difference format of two-dimensional diffusion item is FTCS.

The difference equation for fuel cell (electrolyte, anode and cathode):

$$\begin{aligned}\Delta X \times \Delta Y \times H_{\mathrm{E}} \times \rho_{\mathrm{E}} \times C_{\mathrm{pE}} \times \frac{\mathrm{d}T_{j,k}^{\mathrm{E}}}{\mathrm{d}\tau} &= \Delta X \times \Delta Y \times H_{\mathrm{E}} \times \lambda_{\mathrm{E}} \times \left(\frac{T_{j+1,k}^{\mathrm{E}} - 2 \times T_{j,k}^{\mathrm{E}} + T_{j-1,k}^{\mathrm{E}}}{\Delta X^2} + \frac{T_{j,k+1}^{\mathrm{E}} - 2 \times T_{j,k}^{\mathrm{E}} + T_{j,k-1}^{\mathrm{E}}}{\Delta Y^2}\right) + q_{\mathrm{e}} \times \Delta X \times \Delta Y \times H_{\mathrm{E}} \\ &- \Delta X \times \Delta Y \times K_{\mathrm{EA}} \times (T_{j,k}^{\mathrm{E}} - T_{j,k}^{\mathrm{A}}) - \Delta X \times \Delta Y \times K_{\mathrm{EC}} \times (T_{j,k}^{\mathrm{E}} - T_{j,k}^{\mathrm{C}}) + \Delta X \times \Delta Y \times \frac{i}{2F} \times C_{\mathrm{pco_2}} \times T_{j,k}^{\mathrm{C}} + \Delta X \\ &\times \Delta Y \times \frac{i}{4F} \times C_{\mathrm{po_2}} \times T_{j,k}^{\mathrm{C}} + \Delta X \times \Delta Y \times \frac{i}{2F} \times C_{\mathrm{pH_2}} \times T_{j,k}^{\mathrm{A}} - \Delta X \times \Delta Y \times \frac{i}{2F} \\ &\times C_{\mathrm{pco_2}} \times T_{j,k}^{\mathrm{E}} - \Delta X \times \Delta Y \times \frac{i}{2F} \times C_{\mathrm{pcH_2O}} \times T_{j,k}^{\mathrm{E}} - \frac{\sigma_{\mathrm{B}} \times \Delta X \times \Delta Y \times (T_{j,k}^{\mathrm{E4}} - T_{j,k}^{\mathrm{S14}})}{(1/\varepsilon_{\mathrm{EA}}) + (1/\varepsilon_{\mathrm{s1}}) - 1} \\ &- \frac{\sigma_{\mathrm{B}} \times \Delta X \times \Delta Y \times (T_{j,k}^{\mathrm{E4}} - T_{j,k}^{\mathrm{S24}})}{(1/\varepsilon_{\mathrm{EC}}) + (1/\varepsilon_{\mathrm{s2}}) - 1} \end{aligned} \tag{20}$$

The difference equation for up separator:

$$\begin{aligned}\Delta X \times \Delta Y \times H_{\mathrm{S}} \times \rho_{\mathrm{S}} \times C_{\mathrm{pS}} \times \frac{\mathrm{d}T_{j,k}^{\mathrm{S1}}}{\mathrm{d}\tau} &= \Delta X \times \Delta Y \times H_{\mathrm{S}} \times \lambda_{\mathrm{S}} \times \left(\frac{T_{j+1,k}^{\mathrm{S1}} - 2 \times T_{j,k}^{\mathrm{S1}} + T_{j-1,k}^{\mathrm{S1}}}{\Delta X^2} + \frac{T_{j,k+1}^{\mathrm{S1}} - 2 \times T_{j,k}^{\mathrm{S1}} + T_{j,k-1}^{\mathrm{S1}}}{\Delta Y^2}\right) - \Delta X \times \Delta Y \\ &\times K_{\mathrm{SA}} \times (T_{j,k}^{\mathrm{S1}} - T_{j,k}^{\mathrm{A}}) + \frac{\sigma_{\mathrm{B}} \times \Delta X \times \Delta Y \times (T_{j,k}^{\mathrm{E4}} - T_{j,k}^{\mathrm{S14}})}{(1/\varepsilon_{\mathrm{EA}}) + (1/\varepsilon_{\mathrm{s1}}) - 1} \end{aligned} \tag{21}$$

The difference equation for down separator:

$$\begin{aligned}\Delta X \times \Delta Y \times H_{\mathrm{S}} \times \rho_{\mathrm{S}} \times C_{\mathrm{pS}} \times \frac{\mathrm{d}T_{j,k}^{\mathrm{S2}}}{\mathrm{d}\tau} &= \Delta X \times \Delta Y \times H_{\mathrm{S}} \times \lambda_{\mathrm{S}} \times \left(\frac{T_{j+1,k}^{\mathrm{S2}} - 2 \times T_{j,k}^{\mathrm{S2}} + T_{j-1,k}^{\mathrm{S2}}}{\Delta X^2} + \frac{T_{j,k+1}^{\mathrm{S2}} - 2 \times T_{j,k}^{\mathrm{S2}} + T_{j,k-1}^{\mathrm{S2}}}{\Delta Y^2}\right) - \Delta X \times \Delta Y \times K_{\mathrm{SC}} \\ &\times (T_{j,k}^{\mathrm{S2}} - T_{j,k}^{\mathrm{C}}) + \frac{\sigma_{\mathrm{B}} \times \Delta X \times \Delta Y \times (T_{j,k}^{\mathrm{E4}} - T_{j,k}^{\mathrm{S24}})}{(1/\varepsilon_{\mathrm{EC}}) + (1/\varepsilon_{\mathrm{s2}}) - 1} \end{aligned} \tag{22}$$

ΔX is length of infinitesimal, ΔY is width of infinitesimal, H_{E}, H_{A}, H_{C}, H_{S1}, H_{S2} are the thickness of electrolyte and electrode, the height of anode, the height of cathode, the thickness of up separator and the thickness of down separator, respectively.

4. Simulation and analyses

The fields of temperature, current density and species concentration interfere with each other. To calculate the steady state condition, the fields of temperature, current density and species concentration should be iterated until the results converge. We can obtain the distribution of temperature, current density and gas species concentration of fuel cell at the steady-state point. When the boundary conditions change, the fields of temperature, current density and species concentration change with time

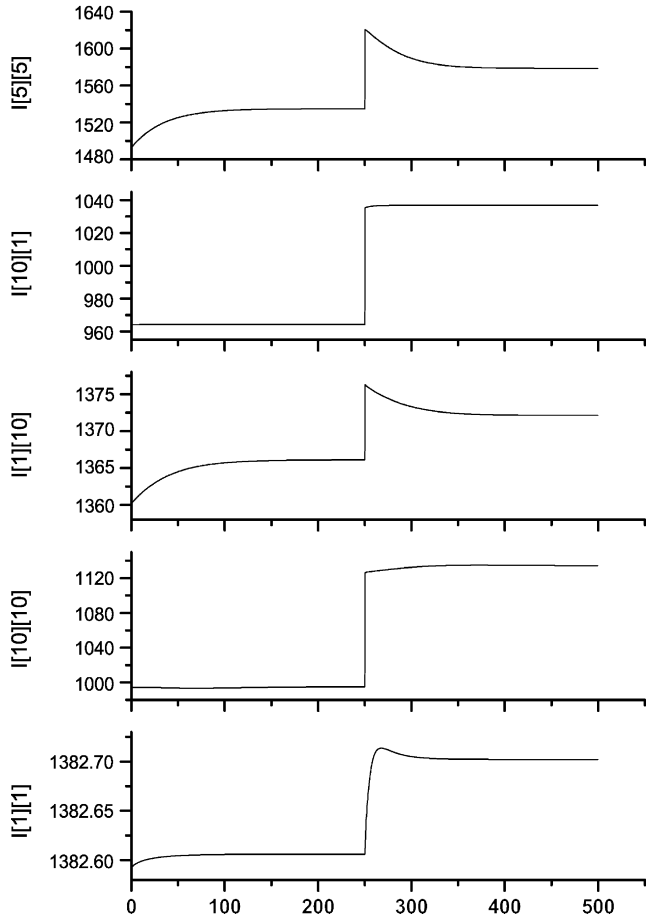

Fig. 2. Dynamic response of the current density.

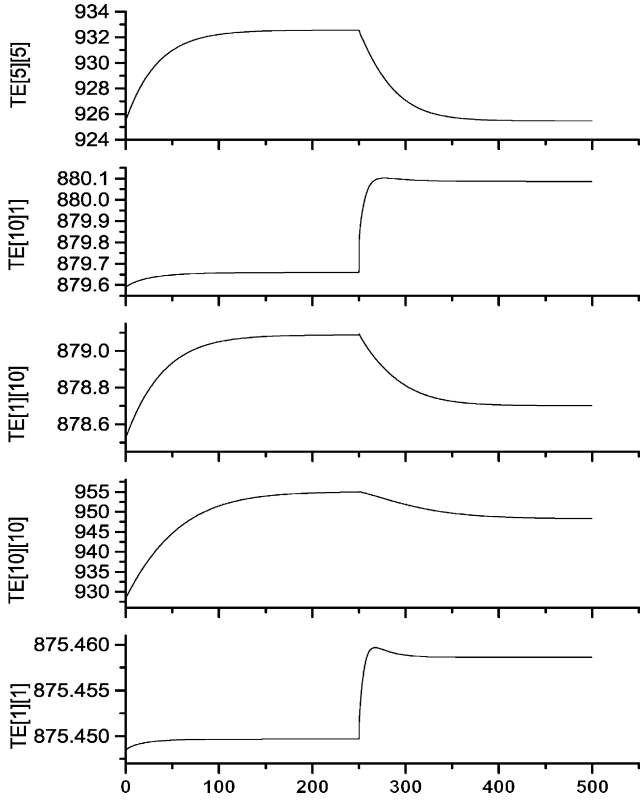

Fig. 3. Dynamic response of the temperature.

correspondingly. They can then reach another steady-state after a period of time.

4.1. Dynamic results and discussions

In our case study, the typical operating conditions were as follows: fuel gas flow rate and inlet temperature 0.017746 mol s^{-1} and 873 K; supplied fuel is composed of 10% CO, 68% H_2, 12% CO_2, 10% H_2O (mole fraction); oxidant (air) flow rate and inlet temperature are 0.1412 mol s^{-1} and 873 K, the oxidant gas is composed of 14.7% O_2, 54.6% N_2, 30% CO_2, 0.7% H_2O (mole fraction), respectively. The temperature of the components in the fuel cell is assumed to be 874 K.

The reaction gas flow into the fuel cell at time of 0 s. It reaches steady-state condition at a time of 100 s. At a time of 250 s, the flow rate of the fuel gas and the oxidant gas step increase 20% at the same time. After about 400 s, fuel cell achieves another steady state. We can obtain the main parameters' two-dimensional field of fuel cell.

Five representative points including $[i=5]$ $[j=5]$, $[i=10]$ $[j=1]$, $[i=1]$ $[j=10]$, $[i=10]$ $[j=10]$, $[i=1]$ $[j=1]$ were selected as examples. The dynamic character of fuel cell can be seen from the dynamic response of the individual parameters at five points.

Fig. 2 shows the dynamic response of the current density of each point. In the initial stage, the current density is increasing because the electrochemical reaction is strengthening gradually. The average current density of the fuel cell is 1440 A m^{-2} when it reaches the steady state after 100 s. At 250 s, the flow rate of the fuel gas and oxidant gas stepwise increase by 20%. It can be seen that the current density then increases quickly due to the increase of species concentration and then decreases slowly under the influence of the temperature. The current density increment at each point is different. The average current density of the fuel cell is 1510 A m^{-2} when it reaches the new steady state. The output power of the fuel cell is increased by about 5%.

Fig. 3 shows the dynamic response of the temperature. From this figure, it can be seen that the temperature of the fuel cell is increasing in the initial stage because of the heat generation of the electrochemical reactions and the resistance. The increase of temperature accelerates the electrochemical reactions. So the current density is increasing and the species concentration is decreasing. The fields of temperature, current density and species concentration reach a steady state after 100 s. But the temperature of each point is different.

After 250 s, the flow rate of the fuel gas and oxidant gas stepwise increase by 20%. The average current density then increases by about 7%. The electrochemical reaction is accelerated. The current density increment of the different points is different and the heat-exchange is uneven. So some points' temperature is increased, others decreased. After 400 s, the field temperature reaches another steady state.

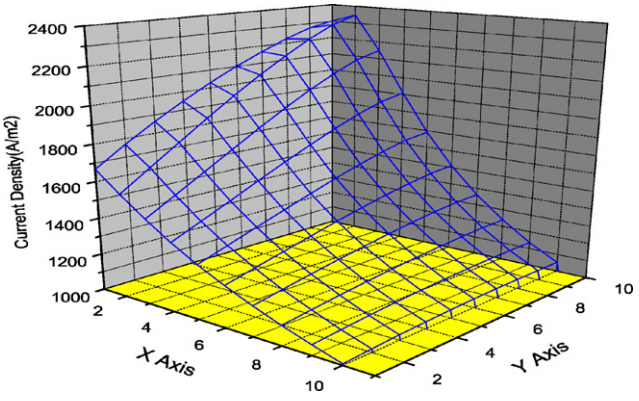

Fig. 4. Two-dimensional field of current density.

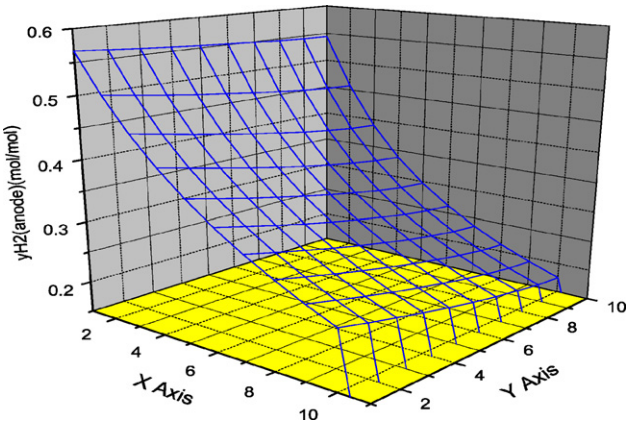

Fig. 6. Two-dimensional H_2 concentration field.

4.2. Steady-state results and discussion

The two-dimensional distribution of current density is illustrated in Fig. 4. It can be seen that the point of maximum current density is located near the inlet of the fuel gas flow and the outlet of the oxidant gas flow. The electrochemical reaction in this region is most intense because of the highest H_2 concentration of the fuel gas and highest temperature of the oxidant gas. The trend in current density is decreasing in the direction of the fuel gas flow and increasing in the direction of the oxidant gas flow.

Fig. 5 reflects the two-dimensional temperature characteristics of the electrolyte. The area of the inlet of the fuel gas flow and the outlet of the oxidant gas flow has the highest temperature because of the most intense electrochemical reactions. It can also be seen that the slope of temperature is sharp in the direction of the oxidant gas flow. The flow rate of the oxidant gas is much greater than that of the fuel gas; the oxidant gas has a very strong cooling effect for the electrolyte. Therefore, the oxidant gas flow rate can be used to control the temperature of the fuel cell.

Fig. 6 shows the two-dimensional H_2 concentration field of the fuel gas. From Fig. 6, it can be seen that the concentration of H_2 decreases in the direction of the fuel gas flow due to the consumption by the electrochemical reaction.

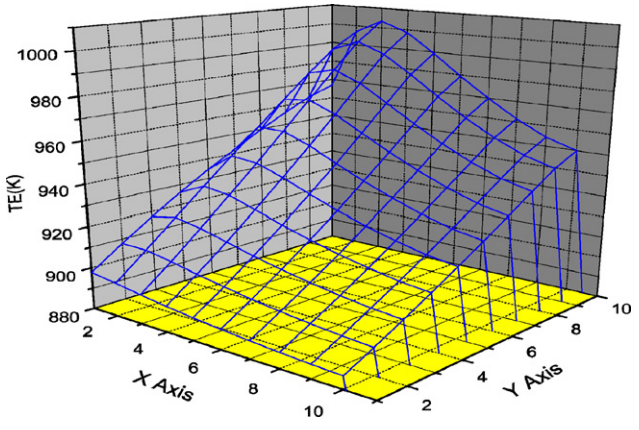

Fig. 5. Two-dimensional temperature field of the electrolyte.

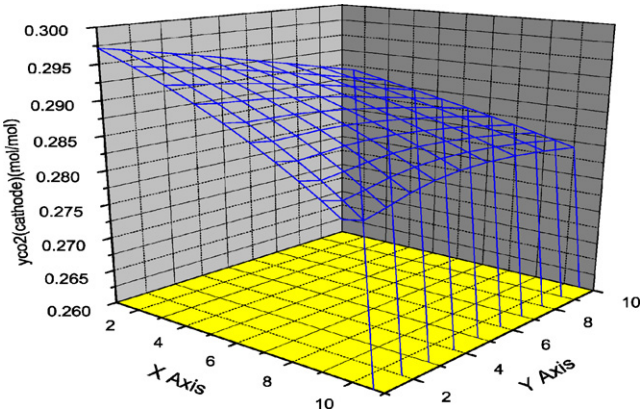

Fig. 7. Two-dimensional CO_2 concentration field of the oxidant gas.

Moreover, the temperature of the oxidant gas increases in the direction of the oxidant gas flow, so that the H_2 concentration of the fuel gas decreases in the direction of the oxidant gas flow.

The CO_2 concentration of the oxidant gas decreases in the direction of the oxidant gas flow because of the consumption by the electrochemical reaction, which can be seen in Fig. 7. In addition, the area of the inlet of fuel gas flow and output of oxidant gas flow has the greatest current density, so the concentration of CO_2 in this region is lower.

5. Conclusions

A two-dimensional dynamic mathematical model of the MCFC in this paper can reflect the distribution of temperature, current density and species concentrations effectively. Moreover, we can obtain the steady state and dynamic characteristics of a cross-flow molten carbonate fuel cell using our simulation model.

It can be seen that the distribution parameters such as temperature, current density and species concentration are affected interactively. This has a very important influence on the safety and efficient operation of the fuel cell.

Acknowledgments

This work was supported by the State Key Fundamental Research Program under the contract No. G1999022303, the National Nature Science Foundation of China (NSFC) under the contract No. 50176031, and FFCSA.

References

[1] H.S. Zhang, S.L. Weng, M. Su, Evaluation of topping and bottoming cycle hybrid power plants with MCFC-micro turbine, ASME TURBO EXPO (2004), GT2004-53397.

[2] W. He, Q. Chen, Three-dimensional simulation of a molten carbonate fuel cell stack under transient conditions [J], J. Power Source 73 (1998) 182–192.

[3] J.-H. Koh, B.S. Kang, H.C. Lim, Effect of various stack parameters on temperature rise in molten carbonate fuel cell stack operation, J. Power Sources 91 (2000) 161–171.

[4] J.-H. Koh, H.-K. Seo, Consideration of numerical simulation parameters and heat transfer models for a molten carbonate fuel cell stack, Chem. Eng. J. 87 (2002) 367–379.

[5] W. He, Dynamic simulation of molten carbonate fuel-cell system, doctor thesis, 2000.

[6] Y. Hua, Numerical simulation heat and mass transfer in a molten carbonate fuel cell, Proc. CSEE 21 (2001) 22–25.